Voltage Stability Enhancement of the Uganda Power System Network

Rebeccah Kyomugisha
Electrical Engineering Department
PAU Institute for Basic Sciences, Technology, and Innovation
Nairobi, Kenya
beckykyomugisha@gmail.com

Christopher Maina Muriithi
Electrical and Electronics Engineering Department
Murangá University of Technology
Murangá, Kenya
cmmuriithi@mut.ac.ke

Milton Edimu
Electrical and Computer Engineering Department
Makerere University
Kampala, Uganda
miltonedimu@yahoo.com

***Abstract*— The unprecedented growth in demand and drive towards deregulation has brought about a complex and constantly changing grid. More so, with the current environmental and economic pressures, there's a reported growing number of numerous transmission and distribution investment deferrals, especially in developing countries. As such, the power system networks are being operated in stressed conditions. Hence, the networks are more prone to voltage instability, and consequently, collapse. Uganda is no exception to these challenges. Thus, a voltage stability assessment of the network is paramount. This research employs the use of Continuation Power Flow (CPF) for the identification of weak regions. Corresponding PV and QV Curves for these buses are also provided to further buttress candidate buses for reactive power compensation. The impact of Static Synchronous Compensators (STATCOMs) on network voltage stability under contingency and fault conditions is also investigated. The results show that with the intervention of STATCOM, an imminent voltage collapse was avoided both during and after fault with bus voltages all restored to normal after incorporation of STATCOM.**

Keywords—Continuation Power Flow, PV Curves, STATCOM, Uganda Power System Network , voltage stability

I. Introduction

The electrical power demand is increasing day-by-day and it is essential to maintain reliable and good quality of the electricity supply [1]. In addition, the current drive towards deregulation and the support of distributed generation has resulted in a constantly changing electric grid [3], [4]. This has resulted in complex interconnected bulk power systems. The attributing factors are the economic and environmental pressures that have led to an increasingly complex system that is operated close to stability limits [5]–[10]. As the system becomes more complex and heavily loaded, voltage instability becomes an increasingly serious challenge. The proof is in the widespread blackouts of the last two decades. Voltage collapse was the causal factor in some of the major blackouts in Greece (July 12, 2004), WSCC, USA (July 02, 1996), West Tennessee (August 22, 1987), and Belgium (August 04, 1982)[7], [11]. It was also a contributing factor in other major blackouts including the 2003 North America blackout and others [12].

The electrical demand in Uganda has been growing at a rapid rate of 10%. This is largely influenced by the high population growth rate. This growth translates to 125,000 new customers every year, with approximately a 2.5million additional on-grid connections projected to have been added in the period 2017 to 2030 [13]. The Government of Uganda is thus, driving efforts to have 100% electricity access by 2040 [14]. As such, over the years, Uganda's generation capacity was expected to have grown to 2500MW by 2020 [15] (actual as of December 2020 was 1268.9 MW [16]) and is expected to grow to over 3000 MW by 2025 [17] to meet the increasing demand and drive towards industrialization [15], [18]–[20]. However, this increase in generation has not been met by a corresponding investment in transmission and distribution infrastructure. As such, the network is heavily constrained and thus, operating in stressed conditions, close to voltage stability and thermal limits. The continued strain on the network results in weak grids which may result in a state of voltage instability, and eventually, voltage collapse which manifests itself by a decline of voltage profiles in one or significant part of the network. Consequently, the network is more prone to blackouts and collapse. In 2020, the network experienced a total of six consecutive nationwide blackouts in the months of April-September alone [21], [22].

This research is therefore intended to provide an assessment of the voltage stability on the Uganda Power Systems Network (UPSN) and corresponding enhancement measures. Specifically, an equivalent model of the network was modeled in MATLAB-PSAT, a continuation power flow analysis performed on the network to establish the state of bus voltages and hence identification of weak buses. PV Curves are also presented to show the impact of increasing loadability on voltage stability. The identified weak regions are noted as candidate buses for the installation of STATCOMs. The impact of this FACTS device is analyzed both in contingency and fault conditions.

II. Voltage Stability Assessment

Whilst voltage stability involves dynamic analysis, power flow-based static analysis methods are often useful for fast approximations. The most commonly used static voltage stability assessment methods are PV and QV curves. PV curves indicate load bus voltage magnitudes versus load active power for a given power factor (pf). For each value of pf, the higher voltage solution indicates a stable voltage case, while the lower voltage lies in the unstable voltage operation zone, according to Equation (1)[23].

$$V = \left[-\frac{2QX + E^2}{2} \pm \frac{1}{2}\sqrt{(2QX - E^2)^2 - 4X^2(P^2 + Q^2)} \right]^{1/2} \quad (1)$$

Where E is V_s (sending end voltage) and V is V_R (receiving end voltage) and E and V are magnitudes with E leading V

Sponsored by the African Union (AU).

978-1-6654-0311-5/21/$31.00 ©2021 IEEE

by δ. P and Q are active power and reactive power respectively.

On the other hand, QV curves provide a more meaningful characteristic for certain aspects of voltage stability, which brings out the sensitivity and variation of bus voltage with respect to reactive power injections (+ve or –ve). QV curves are plots of voltage against the reactive power injected into a bus.

The QV characteristic is plotted on a normalized basis (Q/Pmax, V/E) for various values of P/Pmax. The system is voltage stable in the region where dQ/dV is positive, while the voltage stability limit is reached at dQ/dV = 0 which is also known as the critical operating point. The limiting value of the reactive power transfer at the limiting stage of voltage stability is given by;

$$Q = \frac{V^2}{X} cos2\delta \tag{2}$$

Static voltage stability analysis with these curves involves the identification of nose points by load flow calculations, where the distance between the current operating points and the extremes is the loading margin. These curves indicate proximity to voltage collapse but do not highlight the causes of the voltage instability [7]. The challenge with PV and QV curves arises with power flow convergence as computation approaches the nose points or voltage collapse point.

However, with the Continuation Power Flow (CPF) method, as proposed by Ajjarapu and Christy in [24], we can track a solution branch around the turning point without difficulty [25]. The advantage of CPF is that it provides a complete solution of the nose curve even after reaching the Saddle-Node Bifurcation (SNB) point. The path-following feature of the CPF is captured through a predictor-corrector scheme that adopts locally parameterized continuation techniques to trace the power flow solution paths [26]. An illustration of the CPF process is presented in Fig. 1.

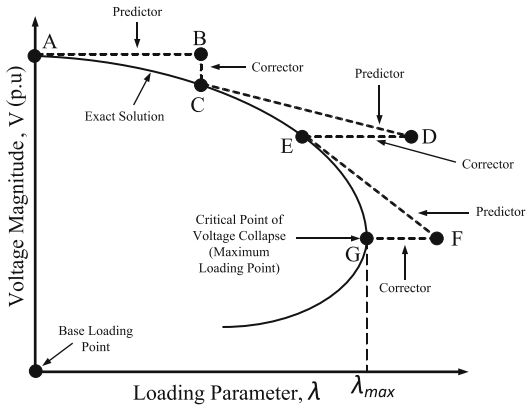

Fig. 1. Continuation Power Flow Process [27]

III. STATCOM FOR VOLTAGE STABILITY ENHANCEMENT

STATCOMs are the most commonly used shunt-connected Flexible AC Transmission Systems (FACTS) devices for power system stability and power quality improvement. A STATCOM utilizes a voltage source converter (VSC) with a pulse with modulation (PMW) controller. The voltage source provides a means of storing DC voltage while at the same time the converter converts it into sinusoidal AC voltage with controllable output and phase angle for reactive power compensation. STATCOMs are known to provide better performance than Static Var compensator (SVC) and have constant current characteristics at low voltages, hence they can provide reactive power compensation even during low voltage grid conditions, unlike shunt capacitors. For the same rating, STATCOMs have a faster response although they are found to incur higher losses and costs than their Static Var Compensator SVC counterparts [28]. Fig. 2 shows a typical STATCOM structure.

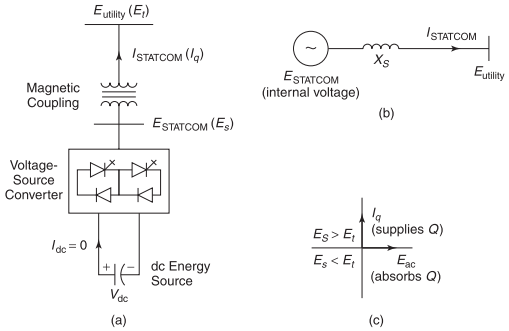

Fig. 2. STATCOM typical structure (a) Power Circuit (b) Equivalent circuit and (c) Power exchange

IV. MATHEMATICAL FORMULATION OF THE CPF ALGORITHM

A. Parameterization

The CPF is performed based on predictor-corrector procedure via the following system of nonlinear equation:

$$F(x) = 0, \tag{3}$$

where

$$x = [\theta, V]^T \tag{4}$$

θ is the vector of the bus voltage angle and V is the vector of the bus voltage magnitudes.

The nonlinear power flow equation in equation (4) is augmented by the loading factor λ as follows:

$$F(x, \lambda) = 0, \qquad 0 \le \lambda \le \lambda_{critical} \tag{5}$$

Where λ = 0 represents the base load condition, and $\lambda = \lambda_{critical}$ represents the critical load.

Equation (5) may be rewritten as;

$$F(\theta, V, \lambda) = 0 \tag{6}$$

B. Predictor scheme

The first task in the predictor process is to calculate the tangent vector. This can be obtained from

$$[F_\theta \; F_v \; F_\lambda] \begin{bmatrix} d\theta \\ dV \\ d\lambda \end{bmatrix} = 0 \tag{7}$$

On the left side of the equation is a matrix of partial derivatives multiplied by the vectors of differentials. The former is the conventional power flow Jacobian augmented by one column (F_λ), whereas the latter $T = [d\theta, dV, d\lambda]^T$ is the tangent vector being sought.

The addition of λ in the power-flow equations introduced an unknown variable. Hence, one more equation is needed to solve the above equations. This is satisfied by setting one of the components of the tangent vector to +1 or -1. This component, referred to as the continuation parameter (CP) imposes a nonzero norm on the tangent vector and guarantees that the augmented Jacobian will be nonsingular at the point of maximum possible system load. Thus, the tangent vector, t is determined as the solution of the linear system.

$$\begin{bmatrix} F_\theta & F_v & F_\lambda \\ & e_k & \end{bmatrix} [t] = \begin{bmatrix} 0 \\ \pm 1 \end{bmatrix} \tag{8}$$

Where e_k is an appropriately dimensioned row vector with all elements equal to zero except the kth, which is equal to one. Once the tangent vector has been found by solving Equation (8), the prediction can be made as

$$\begin{bmatrix}\theta^* \\ V^* \\ \lambda^*\end{bmatrix} = \begin{bmatrix}\theta \\ V \\ \lambda\end{bmatrix} + \sigma \begin{bmatrix}d\theta \\ dV \\ d\lambda\end{bmatrix} \quad (9)$$

where '*' denotes the predicted solution, and σ is a scalar designating step size. After the prediction is made, the next step is to correct the predicted solution.

C. Corrector scheme

In the corrector step, the original set of equations $[F_\theta F_v F_\lambda] = 0$ is augmented by one equation that specifies the state variable selected as the continuation parameter. Thus, the new set of equation is

$$\begin{bmatrix}F(\theta, V, \lambda) \\ X_k - \mu_k\end{bmatrix} = [0] \quad (10)$$

where X_k is the state variable selected as the continuation parameter (CP) and X_k is equal to the predicted value of μ_k.

Slightly modified Newton – Raphson power - flow method can be used to solve these equations. The introduction of the additional equation specifying X_k makes the Jacobian non-singular at the critical operating point. The continuation power-flow analysis can be continued beyond the critical point and thus, obtain solutions corresponding to the lower portion of the P-V curve.

D. Critical point identification

To find the stopping criterion for the continuation power flow, we must determine whether the critical point has been reached. At the critical point, the tangent vector component corresponding to λ is zero (i.e., $d\lambda = 0$) and becomes negative once it passes the critical point. Thus, the sign of the dλ component tells us whether the critical point has been passed or not. Fig. 3 summarizes the CPF processes.

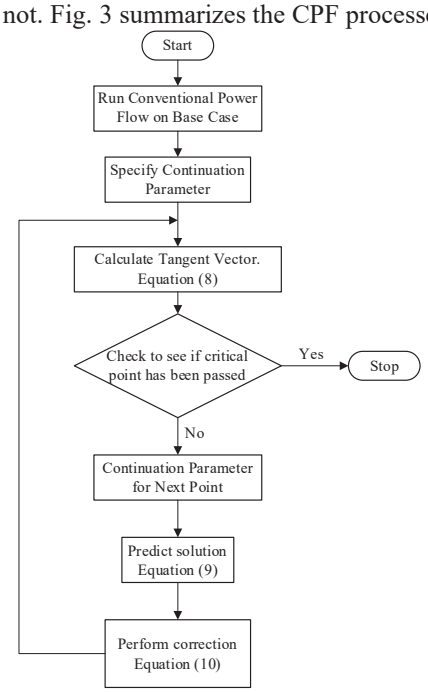

Fig. 3. A flow chart of Continuation Power Flow

V. Results and Discussion

Fig. 6 shows the single line diagram of the modeled Uganda Power Systems Network that was simulated in MATLAB-PSAT. Data used for simulation was for 2019. The network consists of 32 buses, 75 lines, 24-generators, 26 loads, and 7 transformers of 220/132kV.

A. Normal operating conditions (NOC)

At a base of 100MVA, the initial Newton Raphson method was used to solve the load flow. The base case results indicated a total peak load of 841.18MW and 392.48MVaR. From the power flow analysis, 9 buses had their bus voltage magnitudes below 0.9p.u., with the lowest voltages at Bus 15 (Lessos 132kV) - 0.7948p.u. and Tororo 132kV - 0.8387p.u. Fig. 4 indicates the voltage magnitude profile for all buses.

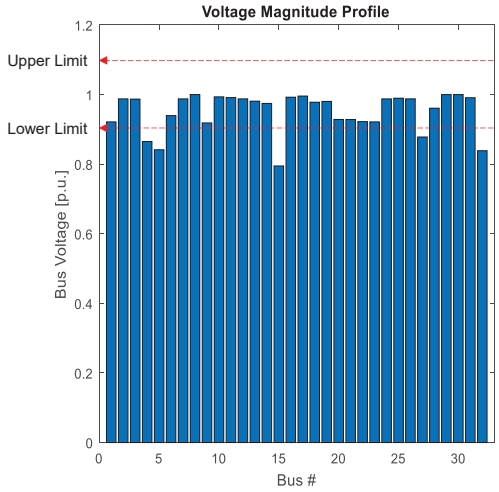

Fig. 4. Voltage profile for the Uganda 32-bus system for NOC

B. Continuation Power Flow

A CPF was performed on the 32-bus system using PSAT. The results highlight the performance of the network with maximum loadability on the system. CPF results indicate that with addition loading up to 1179.25MW (loading parameter of λ =1.4019), the bus voltage magnitudes fall by 4%. Fig. 5 shows the bus voltage profiles after the continuation power flow.

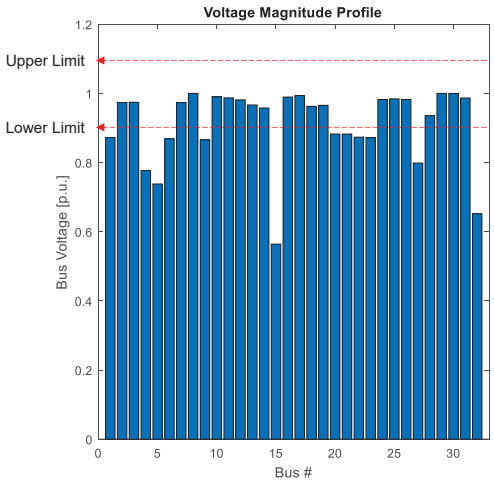

Fig. 5. Voltage profile for the Uganda 32-bus system (CPF)

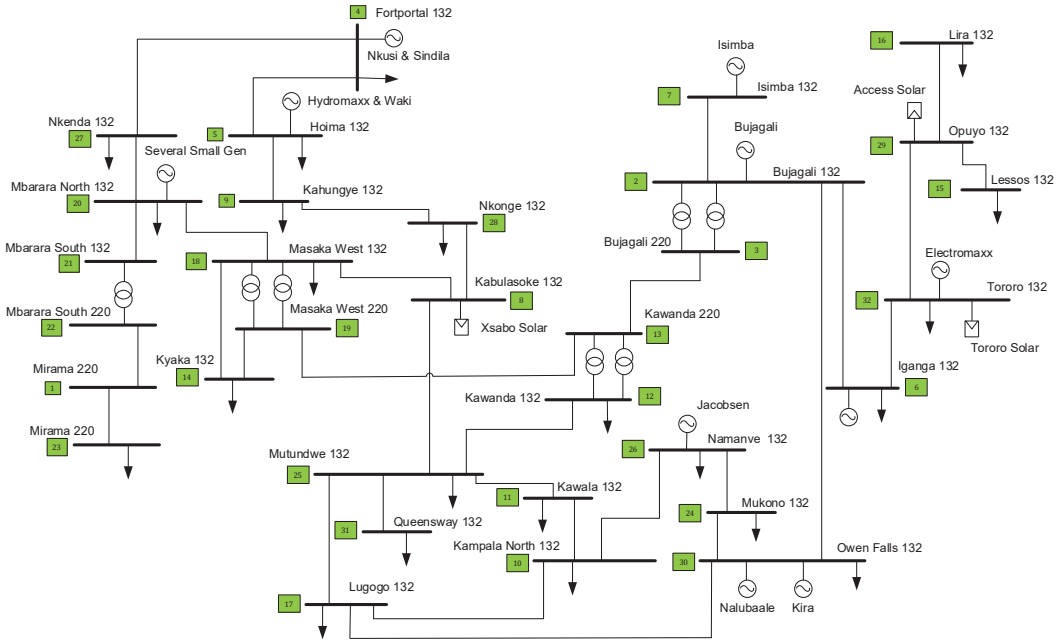

Fig. 6. Single Line Diagram of the modeled 32-bus Uganda Network

The graph indicates that a total of 14 buses have their voltages well below 0.9p.u, with buses 15 (Lessos 132kV), 32 (Tororo 132kV) below 0.7p.u.

A further analysis was performed by plotting the bus PV and QV curves. Fig. 7 and Fig. 8 highlight these results for a few selected weak buses respectively.

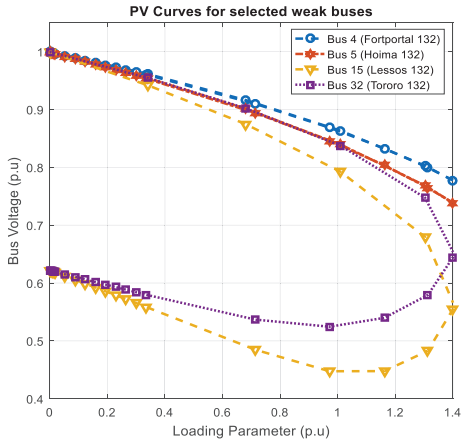

Fig. 7. PV curves for selected weak buses

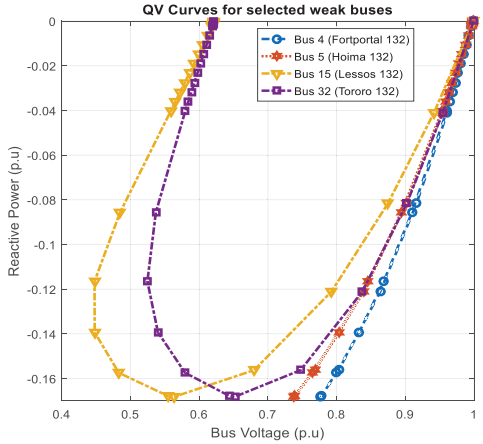

Fig. 8. QV curves for selected weak buses

The CPF analysis shows that Bus 15 (Lessos 132kV) - 0.5639 p.u. and its corresponding interconnecting bus, Bus 32 (Tororo 132kV) - 0.6520 p.u. are the weakest buses on the network. The network's maximum loadability Active and Reactive Powers were 11.7925 p.u and -0.6598p.u respectively.

C. Impact of STATCOM in fault and contingency conditions

A fault was created at Bus 30 (Owen falls 132), which would cause a loss of 380MW of generation at (Kiira Power Station -200MW, and Nalubaale Power Station-180MW). The fault occurred at 1.25s and was cleared at 2s. Fig. 9 shows the performance on Bus 12 and Bus 15, with and without STATCOM. The STATCOMs were placed at three weak buses 32 (Tororo 132) – 30MVaR, 5 (Hoima 132)-20MVaR, and 4 (Fortportal 132)-10MVaR. The sizing was achieved by gradually increasing the rating and monitoring the bus fault performances correspondingly.

The results show that with the intervention of STATCOM, an imminent voltage collapse was avoided during and after faults with bus voltages all restoring to normal after STATCOM had been added.

VI. Conclusion

The study has been able to demonstrate the effectiveness of the CPF method for the identification of weak regions in power systems networks. It is seen that loadability has significant effects on the voltage stability of the network. Hence, loadability effects are observed to be aggravated in fault and contingency conditions. The use of Static Synchronous Compensators for voltage stability enhancement has also been studied.

With the above in mind, this study, therefore, informs us of the following;

- System loading conditions largely influence its voltage stability
- Contingency conditions (loss of line, generation or bus) would aggravate the decline in bus voltages

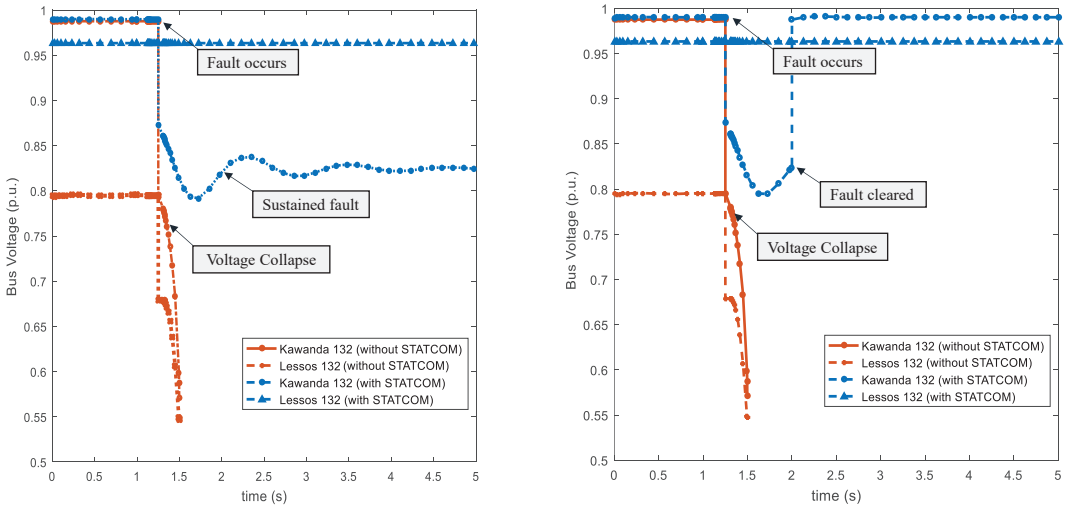

Fig. 9. Bus voltages (a) during fault (sustained fault) and (b) after fault clearance with and without STATCOM

For future studies, the impact of load characteristics on voltage stability can be analyzed. More so, optimization of FACTS sizing and placement can be studied further. Lastly, STATCOM control techniques employing the use of neuro networks or heuristic techniques can be investigated for fast voltage recovery upon occurrence of a disturbance.

ACKNOWLEDGMENT

The authors acknowledge the African Union Commission for funding this research.

REFERENCES

[1] O. Aziz and A. Sandali, *Assessment and analysis of Voltage Stability Indices in electrical network using PSAT Software*. 2016.

[2] S. Rathor and D. Saxena, "Energy management system for smart grid: An overview and key issues," *Int. J. Energy Res.*, vol. 44, Jan. 2020.

[3] Y. Ma, S. Lv, X. Zhou, and Z. Gao, "Review analysis of voltage stability in power system," in *2017 IEEE International Conference on Mechatronics and Automation (ICMA)*, 2017, pp. 7–12.

[4] J. Simpson-Porco, F. Dörfler, and F. Bullo, "Voltage collapse in complex power grids," *Nat. Commun.*, vol. 7, p. 10790, Feb. 2016.

[5] M. Moghavvemi and M. O. Faruque, "Power system security and voltage collapse: A line outage based indicator for prediction," *Int. J. Electr. Power Energy Syst.*, vol. 21, pp. 455–461, Feb. 2013.

[6] B. Shakerighadi, S. Peyghami, E. Ebrahimzadeh, F. Blaabjerg, and C. Back, "A New Guideline for Security Assessment of Power Systems with a High Penetration of Wind Turbines," *Appl. Sci.*, vol. 10, no. 3190, May 2020.

[7] O. Mogaka, R. Orenge, and J. Ndirangu, "Static Voltage Stability Assessment of the Kenyan Power Network," *J. Electr. Comput. Eng.*, vol. 2021, pp. 1–16, Feb. 2021.

[8] S. M. Ashraf, A. Gupta, D. K. Choudhary, and S. Chakrabarti, "Voltage stability monitoring of power systems using reduced network and artificial neural network," *Int. J. Electr. Power Energy Syst.*, vol. 87, pp. 43–51, 2017.

[9] M. S. Danish, T. Senjyu, S. M. Danish, N. R. Sabory, N. K, and P. Mandal, "A Recap of Voltage Stability Indices in the Past Three Decades," *Energies* , vol. 12, no. 8. 2019.

[10] I. G. Adebayo and Y. Sun, "Performance Evaluation of Voltage Stability Indices for a Static Voltage Collapse Prediction," in *2020 IEEE PES/IAS PowerAfrica*, 2020, pp. 1–5.

[11] H. Haes Alhelou, M. E. Hamedani Golshan, T. Njenda, and P. Siano, "A Survey on Power System Blackout and Cascading Events: Research Motivations and Challenges," *Energies*, vol. 12, Feb. 2019.

[12] U. Sultana, A. B. Khairuddin, M. M. Aman, A. S. Mokhtar, and N. Zareen, "A review of optimum DG placement based on minimization of power losses and voltage stability enhancement of distribution system," *Renew. Sustain. Energy Rev.*, vol. 63, pp. 363–378, 2016.

[13] S. de la Rue du Can, D. Pudleiner, and K. Pielli, "Energy efficiency as a means to expand energy access: A Uganda roadmap," *Energy Policy*, vol. 120, pp. 354–364, 2018.

[14] S. Stritzke, P. A. Trotter, and P. Twesigye, "Towards responsive energy governance: Lessons from a holistic analysis of energy access in Uganda and Zambia," *Energy Policy*, vol. 148, 2021.

[15] D. Oweka, M. Edimu, J. Serugunda, and R. Okou, "Optimal Generation Scheduling Approach Applied to the Transmission Grid of Uganda for Enhanced Performance and Cost Reduction," in *2020 IEEE International Conference on Power Systems Technology (POWERCON)*, 2020, pp. 1–6.

[16] Electricity Regulatory Authority (ERA), "Uganda's Electricity Sector Overview," 2020. https://www.era.go.ug/index.php/sector-overview/uganda-electricity-sector (accessed Mar. 20, 2021).

[17] C. Kavuma, D. Sandoval, and H. K. J. de Dieu, "Analysis of power generating plants and substations for increased Uganda's electricity grid access," *AIMS Energy*, vol. 9, no. 1, pp. 178–192.

[18] A. Muwanguzi *et al.*, "Modelling the Growth Trend of the Iron and Steel Industry: Case for Uganda," *Am. J. Ind. Bus. Manag.*, vol. 2020, pp. 1640–1654, Oct. 2020.

[19] J. Mawejje and D. Mawejje, "Electricity consumption and sectoral output in Uganda: an empirical investigation," *J. Econ. Struct.*, vol. 5, Aug. 2016.

[20] G. Okoboi and J. Mawejje, "Electricity peak demand in Uganda: insights and foresight," *Energy. Sustain. Soc.*, vol. 6, Oct. 2016.

[21] The Independent, "Fourth nationwide blackout in five months!," *The Independent*, 2020. https://www.independent.co.ug/fourth-nationwide-blackout-in-five-months/ (accessed Apr. 13, 2021).

[22] Eskom Limited, "Press Releases," 2020. https://www.eskom.co.ug/press-release (accessed Apr. 13, 2021).

[23] D. P. Kothari and I. J. Nagrath, *Modern Power System Analysis*, 4th ed. New Delhi: Tata McGraw Hill, 2011.

[24] V. Ajjarapu and C. Christy, "The continuation power flow: a tool for steady state voltage stability analysis," *IEEE Trans. Power Syst.*, vol. 7, no. 1, pp. 416–423, 1992.

[25] V. Ajjarapu, Ed., "Continuation Power Flow BT - Computational Techniques for Voltage Stability Assessment and Control," Boston, MA: Springer US, 2007, pp. 49–116.

[26] L. Van Dai, N. Minh Khoa, and L. Cao Quyen, "An Innovatory Method Based on Continuation Power Flow to Analyze Power System Voltage Stability with Distributed Generation Penetration," *Complexity*, vol. 2020, 2020.

[27] B. B. Adetokun, C. M. Muriithi, and J. O. Ojo, "Voltage stability assessment and enhancement of power grid with increasing wind energy penetration," *Int. J. Electr. Power Energy Syst.*, vol. 120, 2020.

[28] B. B. Adetokun and C. M. Muriithi, "Application and control of flexible alternating current transmission system devices for voltage stability enhancement of renewable-integrated power grid: A comprehensive review," *Heliyon*, vol. 7, no. 3, 2021.